Diffusion kurtosis imaging: correlation analysis of quantitative model parameters with molecular features in advanced lung adenocarcinoma

Qin Peng[1], Wei Tang[1], Yao Huang[1], Ning Wu[1,2], Lin Yang[3], Ni Li[4]

[1]Department of Diagnostic Radiology, National Cancer Center/National Clinical Research Center for Cancer/Cancer Hospital, Chinese Academy of Medical Sciences and Peking Union Medical College, Beijing 100021, China;

[2]PET-CT Center, National Cancer Center/National Clinical Research Center for Cancer/Cancer Hospital, Chinese Academy of Medical Sciences and Peking Union Medical College, Beijing 100021, China;

[3]Department of Pathology, National Cancer Center/National Clinical Research Center for Cancer/Cancer Hospital, Chinese Academy of Medical Sciences and Peking Union Medical College, Beijing 100021, China;

[4]Office for Cancer Early Diagnosis and Treatment, National Cancer Center/National Clinical Research Center for Cancer/Cancer Hospital, Chinese Academy of Medical Sciences and Peking Union Medical College, Beijing 100021, China.

Abstract

Background: Due to development of magnetic resonance-based functional imaging, it is easier to detect micro-structural alterations of tumor tissues. The aim of this study was to conduct a preliminary evaluation of the correlation of non-Gaussian diffusion kurtosis imaging (DKI) parameters with expression of molecular markers (epidermal growth factor receptor [*EGFR*]; anaplastic lymphoma kinase [*ALK*]; Ki-67 protein) in patients with advanced lung adenocarcinoma, using routine diffusion-weighted imaging as the reference standard.

Methods: Data from patients with primary lung adenocarcinoma diagnosed at Cancer Hospital, Chinese Academy of Medical Sciences (CHCAMS) from 2016 to 2019 were collected for retrospective analysis. The pathologic and magnetic resonance imaging data of 96 patients who met the inclusion criteria were included in this study. Specifically, the K_{app} and D_{app} parameters measured from the DKI model; apparent diffusion coefficient (ADC) value from the diffusion-weighted imaging model; and the *EGFR*, *ALK*, and Ki-67 biomarkers detected by immunohistochemistry and/or molecular biology techniques after biopsy or surgery were evaluated. The relations between quantitative parameters (ADC, K_{app}, D_{app}) and pathologic outcomes (*EGFR*, *ALK*, and Ki-67 expression) were analyzed by Spearman correlation test.

Results: Of the 96 lung adenocarcinoma lesions (from 96 patients), the number of *EGFR*- and *ALK*-positive and high Ki-67 expressing lesions were 53, 12, and 83, respectively. The K_{app} values were significantly higher among patients with *EGFR*-positive mutations (0.81 ± 0.12 *vs.* 0.66 ± 0.10, $t = 6.41$, $P < 0.001$), *ALK* rearrangement-negative (0.76 ± 0.12 *vs.* 0.60 ± 0.15, $t = 4.09$, $P < 0.001$), and high Ki-67 proliferative index (PI) (0.76 ± 0.12 *vs.* 0.58 ± 0.13, $t = 4.88$, $P < 0.001$). The D_{app} values were significantly lower among patients with high Ki-67 PI (3.19 ± 0.69 μm^2/ms *vs.* 4.20 ± 0.83 μm^2/ms, $t = 4.80$, $P < 0.001$) and *EGFR*-positive mutations (3.11 ± 0.73 μm^2/ms *vs.* 3.59 ± 0.77 μm^2/ms, $t = 3.12$, $P = 0.002$). The differences in mean D_{app} (3.73 ± 1.26 μm^2/ms *vs.* 3.26 ± 0.68 μm^2/ms, $t = 1.96$, $P = 0.053$) or ADC values ($[1.34 \pm 0.81] \times 10^{-3}$ mm^2/s *vs.* $[1.33 \pm 0.41] \times 10^{-3}$ mm^2/s, $t = 0.07$, $P = 0.941$) between the groups with or without *ALK* rearrangements were not statistically significant. The ADC values were significantly lower among patients with *EGFR*-positive mutation ($[1.19 \pm 0.37] \times 10^{-3}$ mm^2/s *vs.* $[1.50 \pm 0.53] \times 10^{-3}$ mm^2/s, $t = 3.38$, $P = 0.001$) and high Ki-67 PI ($[1.28 \pm 0.39] \times 10^{-3}$ mm^2/s *vs.* $[1.67 \pm 0.77] \times 10^{-3}$ mm^2/s, $t = 2.88$, $P = 0.005$). K_{app} was strongly positively correlated with *EGFR* mutations ($r = 0.844$, $P = 0.008$), strongly positively correlated with Ki-67 PI ($r = 0.882$, $P = 0.001$), and strongly negatively correlated with *ALK* rearrangements ($r = -0.772$, $P = 0.001$). D_{app} was moderately correlated with *EGFR* mutations ($r = -0.650$, $P = 0.024$) or Ki-67 PI ($r = -0.734$, $P = 0.012$). ADC was moderately correlated with Ki-67 PI ($r = -0.679$, $P = 0.033$).

Conclusions: The K_{app} value of DKI parameters was strongly correlated with different expression of *EGFR*, *ALK*, and Ki-67 in advanced lung adenocarcinoma. The results potentially indicate a surrogate measure of the status of different molecular markers assessed by non-invasive imaging tools.

Keywords: Lung adenocarcinoma; Magnetic resonance imaging; Diffusion kurtosis imaging; Epidermal growth factor receptor; Anaplastic lymphoma kinase; Ki-67 protein

Introduction

Lung cancer remains the leading cause of cancer-related mortality worldwide. The 5-year overall survival rate for all patients diagnosed with lung cancer is relatively low, about 15% to 20% regardless of the tumor stage and treatment received.[1-3] The recognition of specific molecular alterations in certain lung cancer sub-types, has facilitated tailored therapy and ushered in the era of "personalized" oncologic practice in the last decade.[4] Within the family of lung carcinomas, the molecular foundation of lung adenocarcinoma is currently best understood; approximately 60% of all lung adenocarcinomas have an oncogenic driver mutation that, in many cases, predicts treatment response and correlates with certain clinicopathologic features.[5,6]

As for the imaging analysis of lung adenocarcinoma, computed tomography (CT) usually constitutes the first modality in evaluation and staging; other functional modalities such as positron emission tomography-CT or thoracic magnetic resonance imaging (MRI) have emerged to be important supplementary tools.[7] Diffusion-weighted imaging (DWI), one of the widely applied functional MRI techniques, has shown potential for improved cancer detection, prediction of cancer aggressiveness, and evaluation of pathologic sub-types.[8] However, a limitation of DWI is that it works on the assumption that water diffusion is Gaussian in behavior, which is unlikely to be the case in micro-structurally complex tissues.[9] In such tissues, diffusion kurtosis imaging (DKI), a more recently described non-Gaussian technique, potentially better reflects water diffusivity in tissues with ultrahigh b values. The DKI model is sensitive to deviations of tissue diffusion from a Gaussian pattern and has been shown to be robust for parameter quantification, in addition to being more accurate to assess micro-structural complexity in a tissue than conventional DWI.[10] Thus, the application of DKI has been successfully investigated in previous diffusion studies involving various human organs.[11-14]

In the current study, we evaluated the correlation of DKI parameters with the status of micro-structural molecular markers such as epidermal growth factor receptor (*EGFR*), anaplastic lymphoma kinase (*ALK*), and Ki-67 protein to investigate the link between non-invasive imaging parameters and clinicopathologic features, with the aim of providing more valuable information to increase the accuracy of detection, staging, and treatment monitoring for patients with advanced lung adenocarcinoma.

Methods

Ethical approval

This study was approved by the Institutional Review Board of the Cancer Institute & Hospital, Chinese Academy of Medical Sciences (No. NCC2017ZDXM-001) and conducted in accordance with the *Declaration of Helsinki*. Written informed consent was obtained from all patients.

Patients

Between July 2016 and June 2019, a total of 157 consecutive patients diagnosed with lung adenocarcinoma who underwent MRI examination at the Department of Diagnostic Radiology, Cancer Hospital, Chinese Academy of Medical Sciences were included in this study. MRI examinations were performed to evaluate and preoperatively stage these lesions, and the DKI sequence was used for clinical application along with routine conventional MRI. The following inclusion criteria were applied in this study: (1) patients with tumors that were histopathologically confirmed as primary lung adenocarcinomas by subsequent resection or biopsy; (2) patients did not receive any therapy or surgery prior to MRI examination; and (3) patients who underwent routine MRI, DWI, and DKI in the same scanner. The following exclusion criteria were applied: (1) patients with lesions that showed ground-glass opacity (GGO) on MRI; and (2) patients with lesions smaller than 2 cm. Finally, a total of 96 patients (42 males and 54 females) with histopathologically confirmed primary lung adenocarcinoma were enrolled in this retrospective study for data analysis.

Imaging protocol

All MRI scans were performed on a 3.0-T whole-body scanner equipped with a 32-channel coil (Discovery MR750; GE Healthcare, Milwaukee, WI, USA). The routine lung imaging protocol included the following sequences: axial propeller T2-weighted imaging with fat suppression (T2WI/FS), axial fast spin echo T1-weighted imaging, DWI, and DKI. DWI was obtained by using respiratory-gated, single-shot, spin-echo, echo-planar technology with b values of 0, 800 s/mm^2. DKI was performed in the axial plane with b values of 0, 500, 1000, 1500, and 2000 s/mm^2. Details of scanning parameters are shown in Table 1. The scanning range of all sequences was 2 cm above and below the target lesion.

Quantitative image analysis

All images were successfully acquired. Subsequently, parametrical maps of apparent diffusion coefficient (ADC), D_{app}, and K_{app} were calculated on an offline workstation (GE Advantage Workstation AW4.6; GE Healthcare). The mean ADC was determined on the basis of the assumption of a mono-exponential relationship between signal intensity S_b and b value in the DWI model:

$$S(b) = S_0 \times \exp(-b \times ADC)$$

DKI model quantifies the non-mono-exponentiality of the diffusion by means of a second-order Taylor series expansion. To obtain D_{app} and K_{app} parameters, we applied the signal intensity data of five b values based on Rosenkrantz *et al*'s study,[10] using the following equation:

$$S(b) = S_0 \cdot \exp(-bD_{app} + b^2 D_{app}^2 K_{app}/6)$$

Three quantitative parameters, based on the above calculation models, could be partitioned into two categories: diffusion coefficient (D_{app}, ADC) and kurtosis

Table 1: Imaging protocol for DWI and DKI sequences in 157 patients with lung adenocarcinoma.

Parameters	DWI	DKI
Sequence	Single-shot echo planar	Single-shot echo planar
Orientation	Axial bilateral	Axial bilateral
Repetition time (ms)	5900	4200
Echo time (ms)	56	68
Voxel size (mm^3)	$2.0 \times 2.0 \times 4.0$	$2.0 \times 2.0 \times 4.0$
Fat suppression	Spectral adiabatic inversion recovery	Spectral adiabatic inversion recovery
Field of view (mm^2)	384×384	384×384
Matrix	128×128	128×128
Section thickness (mm)	4	4
No. of sections	28	28
No. of signals acquired	2	2
Bandwidth (kHz)	250.0	250.0
Scanning time (min:s)	0:54	4:16
b values (s/mm^2)	0, 800	0, 500, 1000, 1500, 2000

DWI: Diffusion-weighted imaging; DKI: Diffusion kurtosis imaging.

coefficient (K_{app}). Images were analyzed by a radiologist with the experience of interpreting DKI data. The imaging quality was evaluated as adequate or inadequate by the reader before further parameter analysis. Inadequate DKI examinations were mainly caused by (a) excessive motion artifacts; or (b) the high signal barely visible owing to substantial signal loss.[15] The size for each lesion was measured as the average of maximal length and width on the T2WI/FS imaging. Then the reader documented the ADC, D_{app}, and K_{app} values of 96 patients with lung adenocarcinoma on DWI and DKI, respectively. A circular region of interest covering >70% of the maximal lesion area was placed on the T2WI/FS by using freehand selection method and taking care to avoid any cystic components or cavities as well. The identical region of interest was positioned in the corresponding ADC, D_{app}, and K_{app} maps next. The mean ADC, D_{app}, and K_{app} values were automatically measured.

Pathological analysis

Histologic analysis was performed, according to the 2015 World Health Organization Classification of Tumors of the Lung and Pleura,[16] using tissue samples obtained at the time of either surgical resection or image-guided biopsies. In this study, 29 patients underwent surgical resection of the lesion, 52 patients underwent thoraco-scopic surgery, and CT-guided transthoracic core-needle biopsy of lung tumors was performed in 15 patients.

An experienced pathologist evaluated the pathologic sub-types and results of EGFR mutations, ALK rearrange-ments, and Ki-67 protein expression status in all lesions. Genomic deoxyribonucleic acid was extracted from the tumor specimen, and EGFR tyrosine kinase exons 19, 20, and 21 were amplified by a nested polymerase chain reaction (PCR) using specific primers. ALK rearrange-ments were detected by means of fluorescence in situ hybridization or reverse transcription-PCR. Samples were deemed to be fluorescence in situ hybridization-positive if more than 15% of scored tumor cells showed split ALK 5′ and 3′ probe signals or had isolated 3′ signals. Reverse transcription-PCR was used to detect some other specific ALK fusions, for instance, echinoderm microtubule-associated-protein-like 4-anaplastic lymphoma kinase (EML4-ALK). A recent study that investigated the Ki-67 proliferative index (PI) in three large, independent non-small-cell lung cancer cohorts found that the statistically optimal cutoff for classification of lung adenocarcinoma as good and poor prognosis was 25%.[17] Hence, the populations in this study were divided into high-expression (PI ≥ 25%) and low-expression (PI < 25%) groups. These results were collected and reviewed in conjunction with abovementioned imaging parameters.

Statistics analysis

Quantitative variables, tested with the Kolmogorov-Smirnov test for normality analysis and with the Levene test for variance homogeneity analysis, were expressed as mean ± standard deviation. Differences between these sub-groups were compared by using independent-samples t test. Categorical data were presented as counts and percentages, and then sub-groups were analyzed by a Chi-squared test or the Fisher's exact test. Receiver operating characteristic (ROC) curve analysis was performed to calculate the area under the curve (AUC) to determine the accuracy of ADC, K_{app}, and D_{app} in differentiating lesions with different immunohistochemical expression. Sensitivi-ty, specificity, positive predictive value, and negative predictive value were generated using the optimal cutoff values. The diagnostic accuracy could be assessed according to the AUC: excellent, $0.9 < AUC \leq 1.0$; good, $0.8 < AUC \leq 0.9$; fair, $0.7 < AUC \leq 0.8$; poor, $0.6 < AUC \leq 0.7$; fail, $0.5 < AUC \leq 0.6$.[18]

The Spearman correlation analysis was used to evaluate the association of imaging parameters with molecular markers' expression. A correlation coefficient (r) of 1.0 was deemed to indicate perfect correlation; 0.8 to 0.9, strong correlation; 0.6 to 0.7, moderate correlation; 0.3 to 0.5, fair correlation; and lower than 0.3, poor or no correlation.[19] All statistical analyses were carried out using SPSS 23.0 for Windows (IBM SPSS Inc, Chicago, IL,

Table 2: Relationships between the imaging metrics and clinicopathological features of lung adenocarcinomas ($N = 96$).

Characteristics	n	DWI			DKI					
		ADC ($\times 10^{-3}$ mm^2/s)	t	P	D_{app} (μm^2/ms)	t	P	K_{app}	t	P
EGFR mutations			3.38	0.001		3.12	0.002		6.41	<0.001
Positive	53	1.19 ± 0.37			3.11 ± 0.73			0.81 ± 0.12		
Negative	43	1.50 ± 0.53			3.59 ± 0.77			0.66 ± 0.11		
ALK rearrangements			0.07	0.941		1.96	0.053		4.09	<0.001
Positive	12	1.34 ± 0.81			3.73 ± 1.26			0.60 ± 0.15		
Negative	84	1.33 ± 0.41			3.26 ± 0.68			0.76 ± 0.12		
Ki-67 PI			2.88	0.005		4.80	<0.001		4.88	<0.001
High-expression	83	1.28 ± 0.39			3.19 ± 0.69			0.76 ± 0.12		
Low-expression	13	1.67 ± 0.77			4.20 ± 0.83			0.58 ± 0.13		

Data are presented as mean ± standard deviation. ADC: Apparent diffusion coefficient; *ALK*: Anaplastic lymphoma kinase; DKI: Diffusion kurtosis imaging; DWI: Diffusion-weighted imaging; *EGFR*: Epidermal growth factor receptor; PI: Proliferative index.

USA). Two-sided *P* values of <0.05 were considered statistically significant.

Results

General information

Ninety-six lung adenocarcinoma lesions from 96 patients were included with a mean size of 4.1 ± 3.2 cm (range 2.1–7.3 cm). The 96 patients included 42 males (43.8%) and 54 females (56.2%) with a median age of 66 years (44–82 years). Of these, 53 (55.2%) showed *EGFR*-positive mutations, 12 (12.5%) showed *ALK* rearrangements, and 83 (86.5%) showed high Ki-67 expression. In our study, patients with *ALK* rearrangements tended to be younger than those without (78.0% *vs.* 22.0%, $\chi^2 = 4.669$, $P = 0.028$). The two groups displayed no significant difference in the mean size (4.0 ± 2.8 cm *vs.* 4.1 ± 3.1 cm, $t = 1.116$, $P > 0.05$). Two (2.1%) lesions showed both *EGFR* gene mutations and *ALK* gene rearrangements. The most histologic sub-types were lepidic and acinar adenocarcinomas (accounting for 25%, respectively), and rather late pathologic stages of the tumors were recorded (stage IIIA-IV).

Summary of kurtosis metrics

Table 2 summarizes the ADC, K_{app}, and D_{app} metrics in lesions with different immunohistochemical expression.

For the K_{app} values, *EGFR* mutation-positive group was significantly higher than *EGFR* mutation-negative group (0.81 ± 0.12 *vs.* 0.66 ± 0.10, $t = 6.41$, $P < 0.001$); *ALK* rearrangement-negative group was significantly higher than *ALK* rearrangement-positive group (0.76 ± 0.12 *vs.* 0.60 ± 0.15, $t = 4.09$, $P < 0.001$); high Ki-67 expression group was significantly higher than low Ki-67 expression group (0.76 ± 0.12 *vs.* 0.58 ± 0.13, $t = 4.88$, $P < 0.001$).

For the D_{app} values, *EGFR* mutation-negative group was significantly higher than *EGFR* mutation-positive group (3.59 ± 0.77 μm^2/ms *vs.* 3.11 ± 0.73 μm^2/ms, $t = 3.12$, $P = 0.002$); *ALK* rearrangement-positive group was not significantly different from *ALK* rearrangement-negative group (3.73 ± 1.26 μm^2/ms *vs.* 3.26 ± 0.68 μm^2/ms, $t = 1.96$, $P = 0.053$); low Ki-67 expression group was significantly higher than high Ki-67 expression group (4.20 ± 0.83 μm^2/ms *vs.* 3.19 ± 0.69 μm^2/ms, $t = 4.80$, $P < 0.001$).

For the ADC values, *EGFR* mutation-negative group was significantly higher than *EGFR* mutation-positive group ([1.50 ± 0.53] $\times 10^{-3}$ mm^2/s *vs.* [1.19 ± 0.37] $\times 10^{-3}$ mm^2/s, $t = 3.38$, $P = 0.001$); *ALK* rearrangement-positive group was not significantly different from *ALK* rearrangement-negative group ([1.34 ± 0.81] $\times 10^{-3}$ mm^2/s *vs.* [1.33 ± 0.41] $\times 10^{-3}$ mm^2/s, $t = 0.07$, $P = 0.941$); low Ki-67 expression group was significantly higher than high Ki-67 expression group ([1.67 ± 0.77] $\times 10^{-3}$ mm^2/s *vs.* [1.28 ± 0.39] $\times 10^{-3}$ mm^2/s, $t = 2.88$, $P = 0.005$). Representative parametric maps are shown in Figures 1 and 2.

In patients with advanced lung cancer, according to the Spearman analysis, there was a strong positive correlation between K_{app} and *EGFR* mutations or Ki-67 PI ($r = 0.844$, $P = 0.008$; $r = 0.882$, $P = 0.001$, respectively), and a strong negative correlation with *ALK* rearrangements ($r = -0.772$, $P = 0.001$). D_{app} was moderately negatively correlated with *EGFR* mutations or Ki-67 PI ($r = -0.650$, $P = 0.024$; $r = -0.734$, $P = 0.012$), whereas ADC only had moderate negative correlation with Ki-67 PI ($r = -0.679$, $P = 0.033$). The correlations between D_{app} and *ALK* rearrangements, ADC and *EGFR* mutations, ADC and *ALK* rearrangements, were not statistically significant ($P = 0.137$, 0.061, 0.612, respectively).

Table 3 summarizes the AUC for identification of lesions with different immunohistochemical findings for each of the metrics and the optimal thresholds for each of the metrics identified in the ROC analysis. With either scheme, K_{app} had a mildly higher AUC for prediction of adverse final pathologic findings (AUC, 0.79–0.88) than ADC (AUC, 0.49–0.73) or D_{app} (AUC, 0.60–0.86), and differences in performance between the metrics were not significant ($P = 0.183$, $P = 0.734$, respectively). The ROC curves for the three classification schemes are depicted in Figure 3.
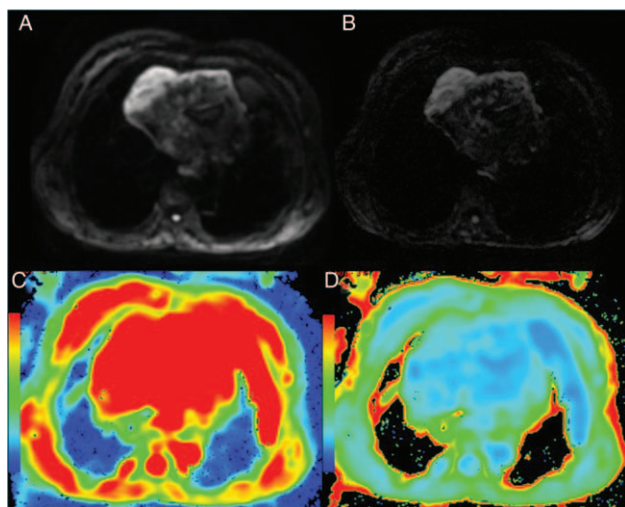
Figure 1: A massive lung adenocarcinoma lesion in the left lung invading mediastinum (*EGFR* mutation positive, *ALK* rearrangement negative, Ki-67 positive, 15%). (A, B) Axial-DWI at $b = 800$, 2000, respectively. (C) Diffusivity maps show decreased signal intensity compared with surrounding tissue, $D_{app} = 3.83 \pm 0.16\ \mu m^2/ms$. (D) Kurtosis maps show increased signal intensity compared with surrounding tissue, $K_{app} = 0.73$. *ALK*: Anaplastic lymphoma kinase; DWI: Diffusion-weighted imaging; *EGFR*: Epidermal growth factor receptor.
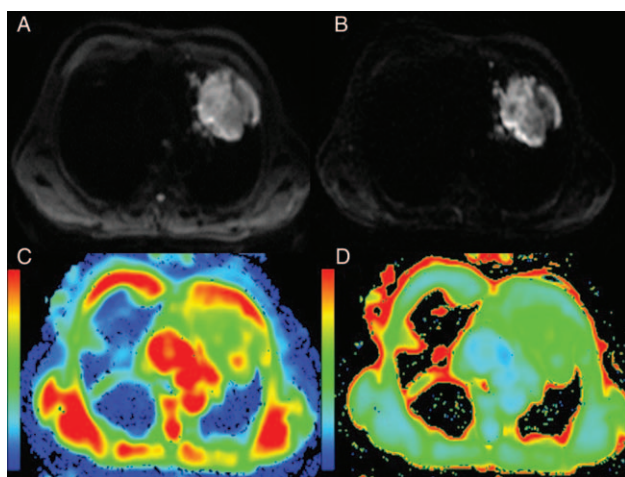
Figure 2: A lung adenocarcinoma lesion in the left upper lobe (*EGFR* mutation in exon 21, *ALK* rearrangement negative, Ki-67 positive, 80%). (A, B) Axial-DWI at $b = 800$, 2000, respectively. (C) Diffusivity maps show decreased signal intensity compared with surrounding tissue, $D_{app} = 3.06 \pm 0.09\ \mu m^2/ms$. (D) Kurtosis maps show increased signal intensity compared with surrounding tissue, $K_{app} = 0.91$. *ALK*: Anaplastic lymphoma kinase; DWI: Diffusion-weighted imaging; *EGFR*: Epidermal growth factor receptor.

Discussion

MRI is an attractive technique that provides an integral assessment of several morphologic and functional techniques to evaluate different tumor characteristics.[20] In the current study, we evaluated DKI-derived parameters to characterize the micro-structural properties of advanced lung adenocarcinomas and correlated them with the corresponding histopathologic findings, to provide a better opportunity for radiologists to potentially gain further insights into the tissue characteristics and improve clinical management triage as compared with the use of standard DWI.

In this study, we found there was a strong positive/negative correlation between kurtosis coefficients (K_{app}) with these molecular markers' status. Besides, the K_{app} values in the *EGFR* mutation-positive group, *ALK* rearrangement-negative group, and high Ki-67 expression group were significantly higher than those in the control groups. Research shows K_{app} represents a unitless parameter, larger K_{app} indicates greater deviation from perfectly Gaussian diffusion behavior,[21] and the K_{app} parameter is likely associated with micro-structural complexity *in vivo*.[22] When a genetic mutation arose in *EGFR* gene, it could have an impact on complicated micro-structures in biologic tissues such as membranes, myelin sheaths, and neural axons, leading to topologic rearrangement and complexity[23,24] reflected by increased kurtosis and hence a higher K_{app} value.[25] As for the Ki-67 antigen, one of several cell cycle-regulating proteins, is proved to be associated with ribosomal RNA transcription, and numerous studies have suggested that tumor cells with high Ki-67 expression exhibited higher cellularity with nuclear atypia.[26-28] Conversely, tumor cells with negative or low Ki-67 expression have loose cellularity and are typically associated with liquefactive necrosis and local fibrosis, resulting in few diffusion barriers.[29,30] The K_{app} parameter represents excessive diffusion kurtosis in the tissue. Thus, it is possible to use differences in K_{app} values observed in our study to reflect the differences in micro-structural irregularity and heterogeneity between these sub-groups.

In addition, a moderate correlation between diffusion coefficient (D_{app} and ADC) and Ki-67 PI or *EGFR* mutations was observed in the study. In the DKI model, D_{app} is an adjusted ADC value that accounts for this non-Gaussian diffusion behavior. In our current study, the D_{app} values were significantly lower among patients with high Ki-67 PI or positive *EGFR* mutations ($P < 0.001$, $P = 0.002$, respectively). It could be explained that the *EGFR* mutation-positive group and high Ki-67 expression group may have an impact on the restriction of water diffusion that can be reflected by decreasing D_{app} values. Further details about this transition remain to be confirmed. In the subsequent ROC analysis for micro-environment assessment, both K_{app} and D_{app} were a little superior to ADC; thus, DKI has been shown to reflect the micro-structural characteristics of adenocarcinoma tissue slightly more accurately than conventional DWI. However, the diagnostic accuracy of these three parameters was not good enough (AUC ranges from 0.49 to 0.88). Upon correlating the D_{app} and ADC values with *ALK* rearrangements, no statistically significant differences were observed with respect to the DKI D_{app} values; however, there was a non-significant trend toward lower D_{app} values among patients with negative *ALK* rearrangements than those with positive rearrangements. The differences in mean D_{app} or ADC values between the groups with or without *ALK* rearrangements were not statistically significant; this may be because of the low rearrangement rate in our study. These results show that the DKI model affords a metric that reflects excess kurtosis in a tissue and contributes to further analysis of molecular biomarkers in lung adenocarcinoma.

Table 3: Receiver operating characteristic analysis of the ADC, D_{app}, and K_{app} values.

Items	EGFR mutations			ALK rearrangements			Ki-67 PI		
	ADC ($\times10^{-3}$ mm²/s)	D_{app} (μm²/ms)	K_{app}	ADC ($\times10^{-3}$ mm²/s)	D_{app} (μm²/ms)	K_{app}	ADC ($\times10^{-3}$ mm²/s)	D_{app} (μm²/ms)	K_{app}
Optimal cutoff	1.23	3.54	0.70	1.11	3.87	0.62	1.21	3.72	0.68
Youden index	0.26	0.41	0.64	0.16	0.43	0.61	0.39	0.78	0.72
Sensitivity (%)	67.44	58.14	86.83	73.81	58.33	94.04	92.35	92.31	79.52
Specificity (%)	58.49	83.02	76.72	41.67	84.50	66.67	47.08	85.54	92.36
PPV (%)	68.89	71.00	82.14	18.52	35.01	61.55	97.54	98.60	98.51
NPV (%)	56.86	73.55	82.53	89.80	93.42	95.26	21.47	50.05	41.44
AUC*	0.66	0.67	0.84	0.49	0.60	0.79	0.73	0.86	0.88
	(0.55–0.77)	(0.56–0.78)	(0.76–0.92)	(0.29–0.69)	(0.36–0.83)	(0.62–0.96)	(0.57–0.88)	(0.73–0.98)	(0.77–0.99)

Cutoff values were obtained by calculating the maximal Youden index: Youden index = sensitivity − (1 − specificity). ADC: Apparent diffusion coefficient; *ALK*: Anaplastic lymphoma kinase; AUC: Area under the curve; *EGFR*: Epidermal growth factor receptor; NPV: Negative predictive value; PI: Proliferative index; PPV: Positive predictive value. *Data in brackets are 95% confidence intervals.
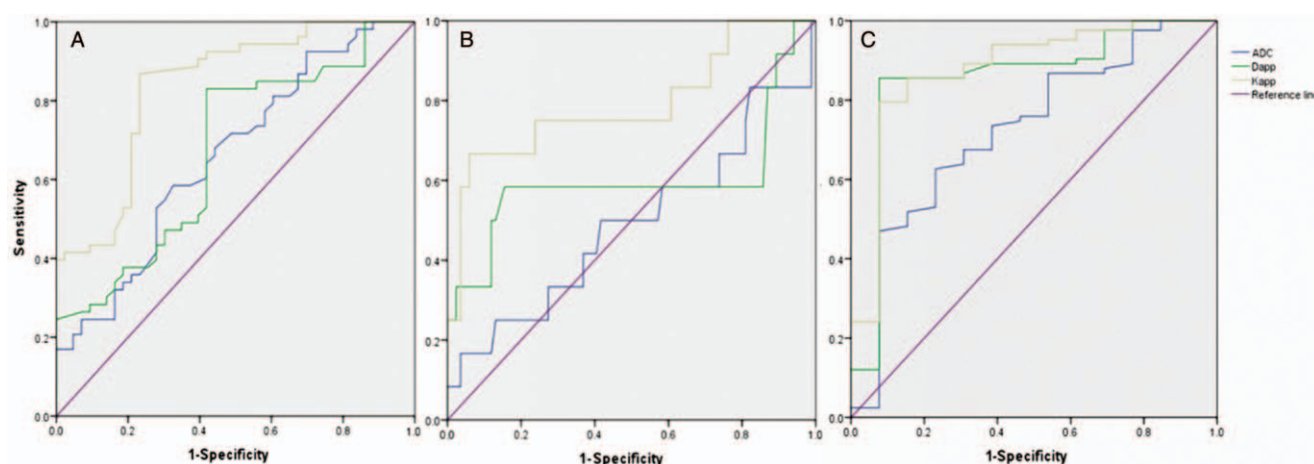
Figure 3: ROC curve based on *EGFR* mutation status (A), *ALK* mutation status (B) and Ki-67 expression (C). *ALK*: Anaplastic lymphoma kinase; *EGFR*: Epidermal growth factor receptor; ROC: Receiver operating characteristics curve.

There were some limitations in this study. First, image quality of small lesions (for example, less than 2 cm) is more easily affected by the patient's heart rate, fluctuation of heart rate, and breathing artifact, causing increased anatomic distortions; hence, our current study focuses on patients with relatively large lesions. Second, MRI scanners in common clinical use were still limited to obtain sufficient signal-to-noise ratio of GGO lesions at ultrahigh *b* value images (>1000 s/mm²), so GGO lesions are not included in this research sample. As a whole, our observations based on a small sampling of MRI examinations are still preliminary, and additional prospective studies are warranted to assess the utility of DKI metrics in predicting clinical outcomes.

We found that the DKI model contains specific information on the non-Gaussian diffusion behavior, provides additional parameters such as K_{app}, as an indicator of immunohistochemical findings, has a high value when assessing the patients with advanced lung adenocarcinomas, and shows slightly better diagnostic accuracies than the conventional DWI model. Using the DKI model during lung MRI is technically feasible in clinical routine, as it provides a practical clinical tool to quantify non-Gaussian water diffusion and probe the microscopic structure of biologic tissues.

Conflicts of interest

None.

References

1. Siegel RL, Miller KD, Jemal A. Cancer statistics, 2019. CA Cancer J Clin 2019;69:7–34. doi: 10.3322/caac.21551.
2. Fukui T, Okasaka T, Kawaguchi K, Fukumoto K, Nakamura S, Hakiri S, *et al*. Conditional survival after surgical intervention in patients with non-small cell lung cancer. Ann Thorac Surg 2016;101:1877–1882. doi: 10.1016/j.athoracsur.2015.11.067.
3. Jakobsen E, Rasmussen TR, Green A. Mortality and survival of lung cancer in Denmark: results from the Danish Lung Cancer Group

2000–2012. Acta Oncol 2016;55 (Suppl 2):2–9. doi: 10.3109/0284186X.2016.1150608.

4. Kim ES, Herbst RS, Wistuba II, Lee JJ, Blumenschein GR Jr, Tsao A, et al. The BATTLE trial: personalizing therapy for lung cancer. Cancer Discov 2011;1:44–53. doi: 10.1158/2159-8274.CD-10-0010.

5. Sholl LM. Biomarkers in lung adenocarcinoma: a decade of progress. Arch Pathol Lab Med 2015;139:469–480. doi: 10.5858/arpa.2014-0128-RA.

6. Papadimitrakopoulou V, Lee JJ, Wistuba II, Tsao AS, Fossella FV, Kalhor N, et al. The BATTLE-2 study: a biomarker-integrated targeted therapy study in previously treated patients with advanced non-small-cell lung cancer. J Clin Oncol 2016;34:3638–3647. doi: 10.1200/JCO.2015.66.0084.

7. Ohno Y, Koyama H, Yoshikawa T, Matsumoto S, Sugimura K. Lung cancer assessment using MR imaging: an update. Magn Reson Imaging Clin N Am 2015;23:231–244. doi: 10.1016/j.mric.2015.01.012.

8. Padhani AR, Liu G, Koh DM, Chenevert TL, Thoeny HC, Takahara T, et al. Diffusion-weighted magnetic resonance imaging as a cancer biomarker: consensus and recommendations. Neoplasia 2009;11:102–125. doi: 10.1593/neo.81328.

9. Le Bihan D. Apparent diffusion coefficient and beyond: what diffusion MR imaging can tell us about tissue structure. Radiology 2013;268:318–322. doi: 10.1148/radiol.13130420.

10. Rosenkrantz AB, Padhani AR, Chenevert TL, Koh DM, De Keyzer F, Taouli B, et al. Body diffusion kurtosis imaging: basic principles, applications, and considerations for clinical practice. J Magn Reson Imaging 2015;42:1190–1202. doi: 10.1002/jmri.24985.

11. Pentang G, Lanzman RS, Heusch P, Müller-Lutz A, Blondin D, Antoch G, et al. Diffusion kurtosis imaging of the human kidney: a feasibility study. Magn Reson Imaging 2014;32:413–420. doi: 10.1016/j.mri.2014.01.006.

12. Sun K, Chen X, Chai W, Fei X, Fu C, Yan X, et al. Breast cancer: diffusion kurtosis MR imaging-diagnostic accuracy and correlation with clinical-pathologic factors. Radiology 2015;277:46–55. doi: 10.1148/radiol.15141625.

13. Pavilla A, Gambarota G, Arrigo A, Mejdoubi M, Duvauferrier R, Saint-Jalmes H. Diffusional kurtosis imaging (DKI) incorporation into an intravoxel incoherent motion (IVIM) MR model to measure cerebral hypoperfusion induced by hyperventilation challenge in healthy subjects. MAGMA 2017;30:545–554. doi: 10.1007/s10334-017-0629-9.

14. Barrett T, McLean M, Priest AN, Lawrence EM, Patterson AJ, Koo BC, et al. Diagnostic evaluation of magnetization transfer and diffusion kurtosis imaging for prostate cancer detection in a re-biopsy population. Eur Radiol 2018;28:3141–3150. doi: 10.1007/s00330-017-5169-1.

15. Glenn GR, Tabesh A, Jensen JH. A simple noise correction scheme for diffusional kurtosis imaging. Magn Reson Imaging 2015;33:124–133. doi: 10.1016/j.mri.2014.08.028.

16. Travis WD, Brambilla E, Nicholson AG, Yatabe Y, Austin J, Beasley MB, et al. The 2015 World Health Organization Classification of lung tumors: impact of genetic, clinical and radiologic advances since the 2004 classification. J Thorac Oncol 2015;10:1243–1260. doi: 10.1097/JTO.0000000000000630.

17. Warth A, Cortis J, Soltermann A, Meister M, Budczies J, Stenzinger A, et al. Tumour cell proliferation (Ki-67) in non-small cell lung cancer: a critical reappraisal of its prognostic role. Br J Cancer 2014;111:1222–1229. doi: 10.1038/bjc.2014.402.

18. Xia J, Broadhurst DI, Wilson M, Wishart DS. Translational biomarker discovery in clinical metabolomics: an introductory tutorial. Metabolomics 2013;9:280–299. doi: 10.1007/s11306-012-0482-9.

19. Akoglu H. User's guide to correlation coefficients. Turk J Emerg Med 2018;18:91–93. doi: 10.1016/j.tjem.2018.08.001.

20. Broncano J, Luna A, Sánchez-González J, Alvarez-Kindelan A, Bhalla S. Functional MR imaging in chest malignancies. Magn Reson Imaging Clin N Am 2016;24:135–155. doi: 10.1016/j.mric.2015.08.004.

21. Jensen JH, Helpern JA. MRI quantification of non-Gaussian water diffusion by kurtosis analysis. NMR Biomed 2010;23:698–710. doi: 10.1002/nbm.1518.

22. Raab P, Hattingen E, Franz K, Zanella FE, Lanfermann H. Cerebral gliomas: diffusional kurtosis imaging analysis of microstructural differences. Radiology 2010;254:876–881. doi: 10.1148/radiol.09090819.

23. Siegelin MD, Borczuk AC. Epidermal growth factor receptor mutations in lung adenocarcinoma. Lab Invest 2014;94:129–137. doi: 10.1038/labinvest.2013.147.

24. Aguirre A, Dupree JL, Mangin JM, Gallo V. A functional role for EGFR signaling in myelination and remyelination. Nat Neurosci 2007;10:990–1002. doi: 10.1038/nn1938.

25. Collier Q, Veraart J, Jeurissen B, Vanhevel F, Pullens P, Parizel PM, et al. Diffusion kurtosis imaging with free water elimination: a Bayesian estimation approach. Magn Reson Med 2018;80:802–813. doi: 10.1002/mrm.27075.

26. Sobecki M, Mrouj K, Camasses A, Parisis N, Nicolas E, Llères D, et al. The cell proliferation antigen Ki-67 organises heterochromatin. Elife 2016;5:e13722. doi: 10.7554/eLife.13722.

27. Karaman A, Durur-Subasi I, Alper F, Araz O, Subasi M, Demirci E, et al. Correlation of diffusion MRI with the Ki-67 index in non-small cell lung cancer. Radiol Oncol 2015;49:250–255. doi: 10.1515/raon-2015-0032.

28. Chirieac LR. Ki-67 expression in pulmonary tumors. Transl Lung Cancer Res 2016;5:547–551. doi: 10.21037/tlcr.2016.10.13.

29. Rosenkrantz AB, Prabhu V, Sigmund EE, Babb JS, Deng FM, Taneja SS. Utility of diffusional kurtosis imaging as a marker of adverse pathologic outcomes among prostate cancer active surveillance candidates undergoing radical prostatectomy. AJR Am J Roentgenol 2013;201:840–846. doi: 10.2214/AJR.12.10397.

30. Bodey B, Bodey B Jr, Gröger AM, Siegel SE, Kaiser HE. Clinical and prognostic significance of Ki-67 and proliferating cell nuclear antigen expression in childhood primitive neuroectodermal brain tumors. Anticancer Res 1997;17:189–196.